Wide-Area RTK

High Precision Positioning on a Continental Scale

Real-time corrections at the decimeter level over an entire continent? The challenge lies in minimizing the ranging errors from signals propagating through the Earth's atmosphere. European researchers describe how it can be done using a Wide Area Real-Time Kinematic concept that exploits the full geometry of the observations, a central processing facility, and undifferenced processing of measurements from widely space GNSS reference receivers to create a real-time ionospheric model of the signal slant delays.

MANUEL HERNÁNDEZ-PAJARES, J. MIGUEL JUAN, JAUME SANZ, ANGELA ARAGON-ANGEL, PERE RAMOS-BOSCH
RESEARCH GROUP OF ASTRONOMY AND GEOMATICS, UNIVERSITAT POLITÈCNICA DE CATALUNYA (GAGE/UPC) AND GAGE-NAV S.L.
JARON SAMSON, MICHEL TOSSAINT, MICHELANGELO ALBERTAZZI
ESTEC/ESA
DENNIS ODIJK
CURTIN UNIVERSITY OF TECHNOLOGY
PETER J. G. TEUNISSEN
CURTIN UNIVERSITY OF TECHNOLOGY AND DELFT INSTITUTE OF EARTH OBSERVATION AND SPACE SYSTEMS
PETER DE BAKKER, SANDRA VERHAGEN, HANS VAN DER MAREL
DELFT INSTITUTE OF EARTH OBSERVATION AND SPACE SYSTEM

This Envisat mosaic was produced using images acquired by Envisat's Medium Resolution Imaging Spectrometer (MERIS) instrument. ESA photo

A common assumption in real-time kinematic (RTK) techniques is that the differential ionospheric delay between a GNSS transmitter and each of the roving or reference receivers is negligible. However, increased position uncertainty — spatial decorrelation — is usually allocated to the baseline receivers as baseline distances increase.

A refinement of this assumption comes with the network RTK (NRTK) using a set of permanent receivers to mitigate atmospheric dependent effects, such as the ionospheric delay, over distance.

These two approaches work well for baselines up to 10-20 kilometers (RTK) and to 50–70 kilometers (NRTK), requiring only one extra equation per satellite in-view. They both allow quick carrier phase ambiguity fixing and the corresponding real-time sub-decimeter error level positioning for high precision applications such as civil engineering. But both techniques restrict themselves to satellites with fixed double-differenced ambiguities, without exploiting the full geometry of the observations in a real-time ionospheric model of the slant delay.

The WARTK concept was introduced in the late 1990s to address these deficiencies. The method dramatically increases the RTK/NRTK service area, with permanent stations separated by up to 500–900 kilometers — all while requiring 100 to 1,000 times fewer receivers covering a given region.

This is accomplished thanks to combining at a Central Processing Facility (CPF) new ionospheric tomography and travelling ionospheric disturbance models with real-time geodetic undifferenced processing of measurements

from widely separated permanent GNSS receivers, which is able to provide to the users undifferenced accurate ionospheric corrections that are used as additional information with its corresponding estimated standard deviation.

An example of such a permanent receiver network is the network of European Geostationary Navigation Overlay Service (EGNOS) ranging and monitoring station (EGNOS RIMS). This service would be able to provide WARTK corrections to navigation users, resulting in typical accuracies of around 10 centimeters of error, within a short convergence time. The availability of precise ionospheric corrections helps to decisively fix the real-time carrier phase ambiguities of the WARTK user.

Over the last 10 years, many experiments demonstrated the feasibility of WARTK using both actual and simulated data, while the technique evolved.

This article summarizes the present state and key results of the WARTK technique. We discuss the expected performance of future multi-frequency/multi-constellation GNSS scenarios using both WARTK CPF and associated products, including WARTK user accuracy, convergence time, and integrity. We detail our analysis using recently simulated multi-frequency Galileo data derived from a number of R&D projects funded by the European Space Agency (ESA).

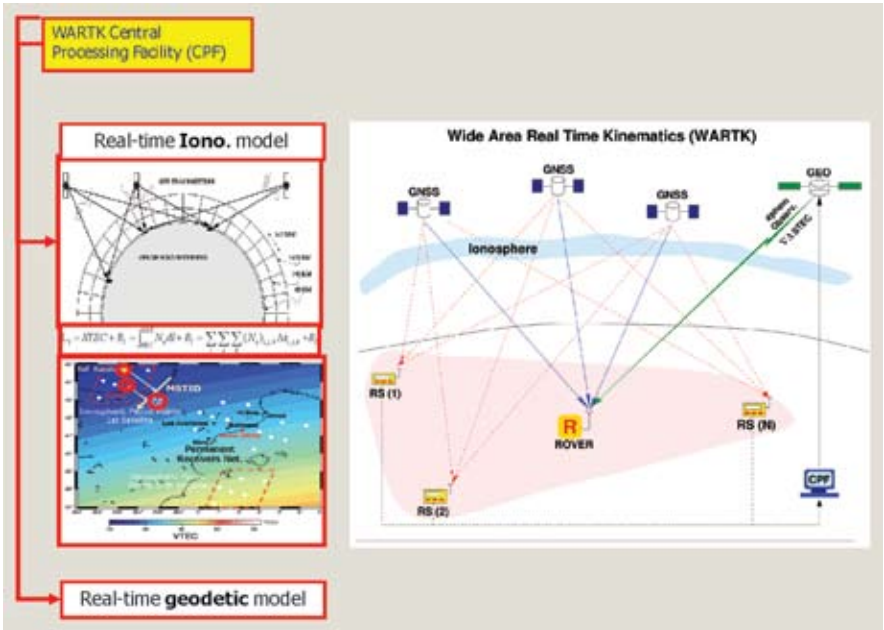

FIGURE 1 Layout representing the main components of the WARTK system: The Central Processing Facility (CPF), continuously running the combined geodetic and ionospheric models (this with both tomographic and Medium Scale Travelling Ionospheric Disturbance components), both feed with the measurements of the permanent stations (red circles). The WARTK CPF provides the accurate ionospheric corrections and remaining information necessary to the WARTK user (blue circle), in order to be able to navigate with the carrier phase at decimeter error level.

Background to WARTK

ESA has been funding several R&D projects to evaluate the feasibility of a future high-precision positioning service based on a new augmentation system. Data gathered by the existing EGNOS RIMS — originally designed to guarantee integrity in safety-of-life GNSS usage for civil aviation — would feed into this service.

Several projects carried out since 2000 have focused on finding accurate ways of modeling the ionosphere in real-time, profiting from the well-known coordinates of the permanent RIMS receivers. To date, this has been done only notionally by processing data from permanent receivers at the network's central processing facility (CPF) and roving receivers (users), emulating real-time conditions. In these trials, the typically static receivers of users are treated as roving ones, as well as occasionally truly roving.

A future Wide Area RTK (WARTK) system would extend the sub-decimeter error level for GNSS navigation across continental regions and reduce the cost of existing high-precision positioning applications such as civil engineering, while creating opportunities for new applications.

Ionospheric delay of GNSS signals is the main source of error that limits the extension of classical high-precision service despite use of such techniques as real-time kinematic (RTK) positioning, virtual reference stations (VRS) or Network RTK (NRTK). For distances of a few tens of kilometers, the assumption of either a negligible or constant differential ionospheric delay between the multi-frequency roving receiver and the closer reference receiver is not valid.

Moreover, we cannot use this assumption in such techniques as a valuable additional condition to solve the carrier phase ambiguity in real-time for a position accuracy of ten or less centimeters. For distances greater than 100 kilometers, real-time ambiguity fixing challenges even permanent receivers.

The WARTK technique, introduced 10 years ago solves this problem by introducing a precise real-time algorithm to provide GNSS multifrequency users with accurate ionospheric estimations in the core of its real-time carrier phase ambiguity fixing. (See the papers by M. Hernández-Pajares et alia 1999a and O. Colombo et alia listed in the Additional Resources section near the end of this article.) This approach also supports associated precise navigation in the context of undifferenced or space state representation.

The ionospheric model running in the WARTK CPF referred to in **Figure 1** precisely captures the real-time, linear and larger scale electron content variations. The model tomographically maps the ionospheric state as measured by a network of permanent GNSS receivers, each separated up to many hundreds of kilometers.

A second component of the model, needed to provide precise ionospheric corrections to the users, characterizes and mitigates ionospheric waves (also called *medium scale traveling ionospheric*

FIGURE 2 Map representing the simulated scenario, with GNSS permanent stations (red squares), IGS-station Stavanger (green triangle) and GNSS users (white flags).

disturbances or MSTID), which are a frequent non-linear phenomenon affecting GNSS users at mid latitude.

To this end, another simple but efficient model that mitigates the MSTIDs was developed, as described in the papers by M. Hernández-Pajares et alia (2006a-b). This precise real-time ionospheric model is well integrated in the geodetic filter and ensures successful ambiguity fixing among the permanent GNSS stations and especially between the roving user and the nearest permanent site.

Once the user ionospheric corrections are applied by the user, cycle ambiguities can be fixed either by using a three-carrier ambiguity resolution (TCAR) approach or the well-known LAMBDA method, which has been used for the successful ambiguity resolution in the single-epoch ambiguity section. (See the article by P. J. G. Teunissen, 1995, listed in Additional Resources.) This method is numerically efficient, can be applied to other GNSSes, and provides the highest possible success rate of all ambiguity resolution methods.

The WARTK technique thus described typically provides an accuracy within 10 centimeters quickly with assured integrity, as confirmed in recent research activities supported by ESA. (See, for example, the papers by M. Hernández-Pajares *et alia* 2008 and 2009.) These activities have been focused on establishing the feasibility of WARTK, not only at the positioning level but also, for the first time, at the integrity level.

Over the past 10 years more than 10 WARTK measurement campaigns have been carried out using either simulation or real GPS data. These incorporated various combinations of GNSS signals, baseline-lengths, ionospheric conditions, and user dynamics. And they demonstrated the feasibility of the WARTK technique for both actual dual-frequency and simulated three-frequency data.

GNSS RF Simulator Experiment

In order to investigate the feasibility of WARTK feasibility using multiple constellations and multi-frequency signals, we first defined a representative network of permanent GNSS receivers to generate the WARTK corrections for the users. This step was needed in order to generate realistic signals from which to gather corresponding measurements, with various error sources emulating as much as possible actual conditions.

The three main elements — network design and user characteristics, signal simulation setup, and additional error sources — may be summarized as follows.

First we defined a set of permanent GNSS receivers. Because the ionospheric model constitutes the primary factor with which to build the precise corrections needed to navigate with errors of about 10 centimeters, the distribution of the receivers is critical.

The red squares in **Figure 2** represent the simulated receiver distribution, which included seven actual EGNOS RIMS receiver locations. Additionally, we included an International GNSS Service (IGS) receiver at Stavanger, Norway, represented in the figure by a green triangle. These receivers were typically separated by 400–800 kilometers.

Next, two roving receivers were simulated, one located at Delft, the Netherlands, and the other in Dunkerque, France. Although they correspond to actual permanent IGS receivers, we treated them as real-time roving users in the experiment analysis. We used the nearer permanent network receiver in Swanwick (RIMS A015) as a reference for double-differenced ambiguity fixing, while the rovers were several hundreds of kilometers away — in Dunkerque 257 kilometers away, and Delft at 413 kilometers.

As illustrated in **Figure 3**, the measurement test-bench was set up at ESA/ESTEC European Navigation Laboratory (ENL) and included two GNSS simulators to generate the GPS and Galileo signals and a GPS+Galileo multi-frequency receiver to track these signals.

We selected measurements and simulation options that would resemble an actual multi-frequency Galileo+GPS scenario of the future as closely as possible:

- *Observables* — carrier phase and pseudoranges associated with E1, E5a, E5b (Galileo) and L1, L5 (GPS) signals.
- *Slant ionospheric delay* — simulated using the climatological model from the International Reference Ionosphere (IRI) in mid-solar cycle conditions from year 1993. The left plot in Figure 4 illustrates the vertical ionospheric delay over the receivers.
- *Tropospheric delay* — simulated using a modified Hopfield model, which is notably different from the Niell model used for estimating tropospheric retrieval.
- *Multipath* — derived from actual GPS measurements and compatible with actual GIOVE measurements

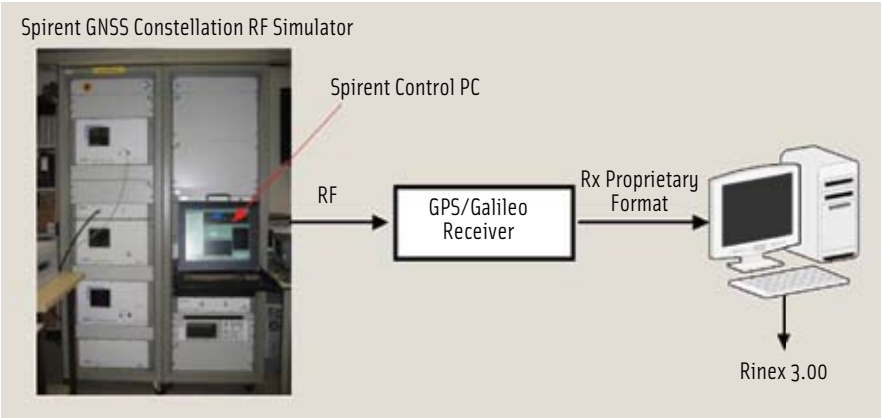

FIGURE 3 **Simulation and Data Collection Test-Bench**

(See paper by M. Hernández-Pajares et alia, 2009), such as those recorded in the article by A. Simsky et alia — note the right plot in **Figure 4**.) These values have been included at the most sensitive point: the pseudorange user measurements.

Central Processing Facility

Similar to the GPS Master Control Station or the EGNOS processing facility, the WARTK Central Processing Facility has the fundamental mission of generating in real-time the required WARTK user products for the precise, fast, and reliable navigation. One important difference, however, is that the WARTK user's real-time positioning is based on the carrier phase measurements and precise modeling. Moreover, a user's real-time ambiguity fixing (or constraining) is closely linked to the availability of very precise ionospheric corrections, to be provided as well by the WARTK CPF (Figure 1).

In order to characterize the suitability of the geodetic and ionospheric models, the plots in **Figures 5a** to **5d** show that the post-fit residuals of the main geodetic measurement, or iono-free combination of carrier phases, are compatible with the required centimeter-level accuracy. They are just slightly better when a dual-layer ionospheric model is used, shown in Figure 5(a) for individual residuals and 5(b) for root mean square (RMS) values.

However, the effect is dramatic when the ionospheric phase combination is analyzed in Figure 5(c) and 5(d), where the dual-layer ionosphere model diminishes the post-fit RMS residual by a factor of five. This example is very similar to the best ideal case when no ionosphere has been simulated in the data. The improvement is attributable to the 3D modeling of the dual-layer ionosphere (actually 4D because the time dependence is modeled in the Kalman filter), instead of the simpler 2D model using a single-layer ionosphere (as was demonstrated in the article by M. Hernández-Pajares et alia 1999b).

This computation of the total electron content is more accurate because it more closely reflects the actual structure of the ionospheric free electron distribution as "seen" by ground GNSS receivers.

Figure 6 illustrates the error of two WARTK CPF outputs, the receiver and satellite clocks, this one an additional important WARTK CPF product required for undifferenced precise positioning, represented for both Galileo and GPS constellations.

In particular receiver clocks performed well, with errors less than two centimeters, compatible and somehow better compared with the results being obtained in real-time from GPS data, such as the ones reported in the article by J. M. Juan et al. (2009), at the level of five centimeters, and approaching the level of the better estimations of the IGS Real Time Working Group. (The

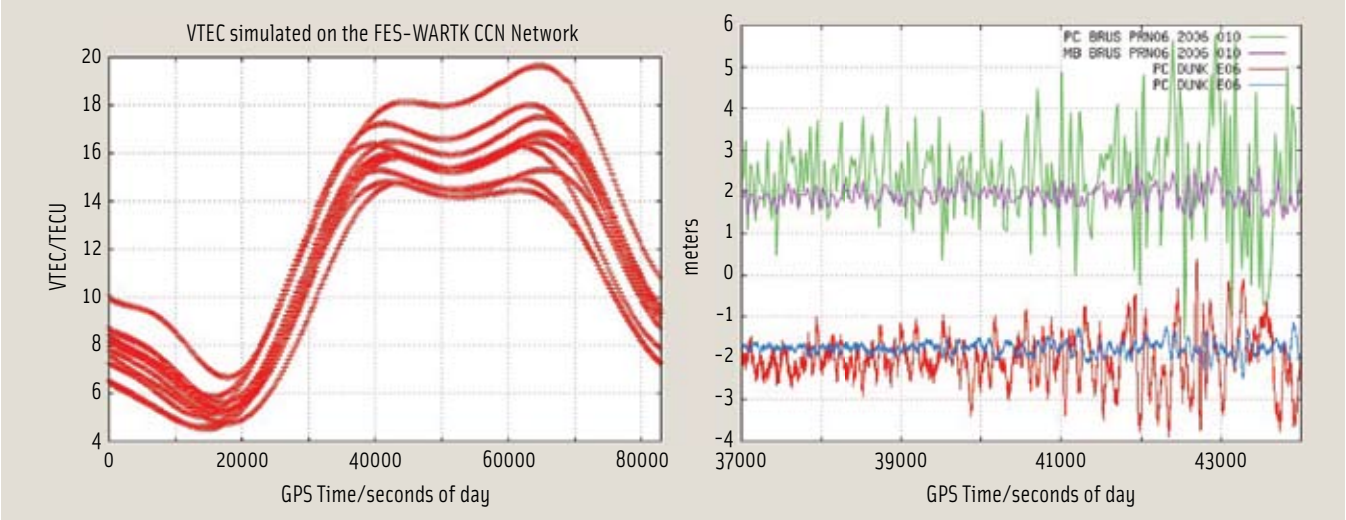

FIGURE4 **Left plot: Vertical total electron content (in TECUs) over the various receivers involved in the experiment. Right plot: Actual multipath error in meters in ionospheric-free (PC, green) and Melbourne-Wübbena combinations (MW, magenta), compared with the adopted one in the simulation (red and blue, correspondingly).**

slightly better results here are related with a slightly optimistic model of measurement noises and orbit error, among a larger number of satellites in view in the multi-constellation scenario.)

The vertical troposphere residual delay is another unknown, which must be estimated as a random walk in the WARTK CPF filter. Tropospheric delay error is driven down below one centimeter, converging within 10 minutes, as shown in **Figure 7**. This result agrees with previous experimental results using actual data and meets the required accuracy. Moreover, the system converges somewhat more quickly using a dual-layer ionosphere model, instead of a single layer model.

Finally, the WARTK CPF fixes as many phase ambiguities as possible, in order to send accurate real-time ionospheric delay values to the users, which are used as a valuable real-time constraint to speed up the convergence of their own ambiguities. At the same time the ambiguity fixing between permanent stations also helps the accuracy of real-time orbits and clocks, as is confirmed in J. M. Juan et alia (2009). Experimental results shown in **Figure 8** indicate that more than 85 percent of wide-lane and narrow-lane ambiguities are fixed.

Finally, **Figure 9** shows the performance of the slant total electron content

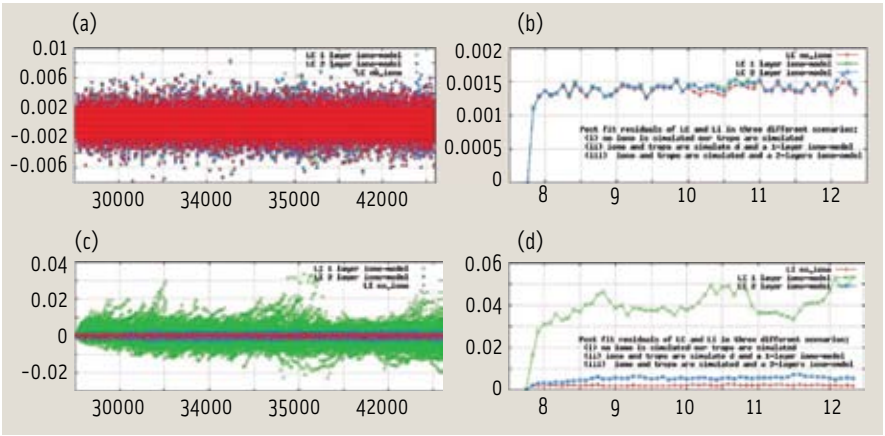

FIGURE 5 (a) Individual post-fit residuals (meters) for first order iono-free (LC) carrier phase vs. GPS time (seconds) (b) Individual post-fit residuals for geometric-free (LI) for single, dual layer ionospheric model estimation and no simulated ionosphere (meters) versus GPS time (seconds). (c) RMS for first order iono-free (LC) carrier phase (meters) vs. GPS time (hours) and (d) RMS for geometric-free (L1) for single and dual-layer ionospheric models and non simulated ionosphere (meters) vs. GPS time (hours). Note: In the case when no simulated iono was considered, the ionospheric model has been also estimated with a dual layer-model.

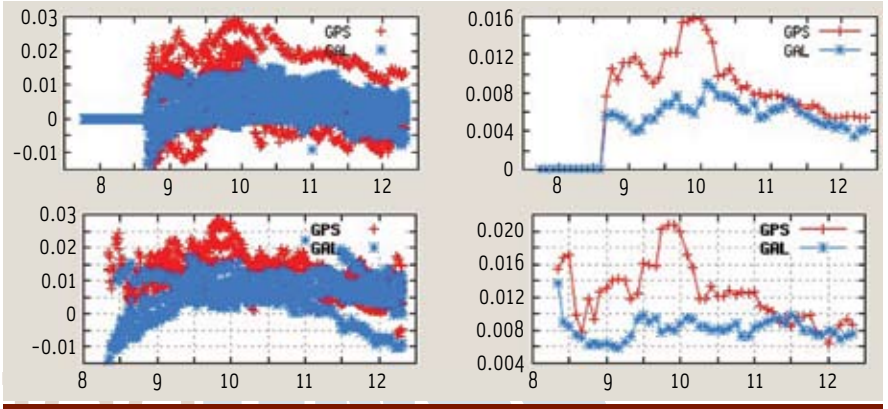

FIGURE 6 Left plots: individual receiver error (top) and individual transmitter clock error (bottom), in meters, as function of the time of the day in hours. Right plots: similar representation for receiver error RMS (top), and transmitter clock RMS (bottom). Errors were determined by the WARTK CPF, estimating the ionospheric delay with a dual-layer ionospheric model.

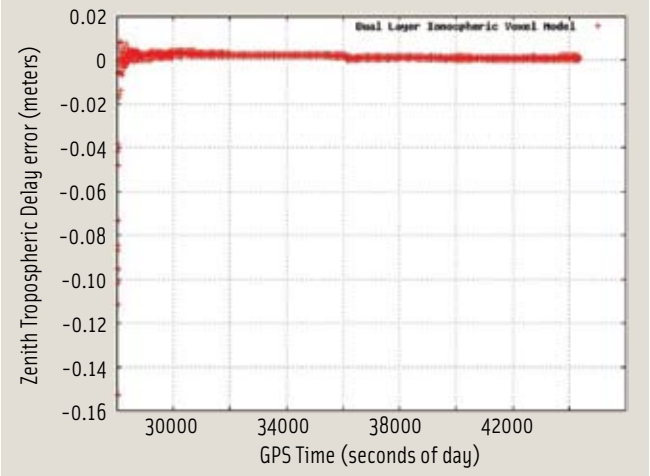

FIGURE 7 WARTK CPF zenithal tropospheric delay error in terms of the time in seconds of day, for a dual-layer ionospheric model.

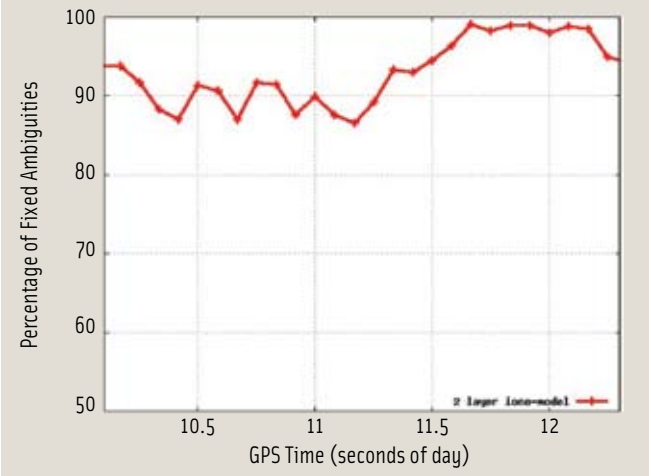

FIGURE 8 Relative percentage of WARTK CPF phase ambiguity fixing (wide-lane and short-lane combinations) in terms of the time of the day, in hours

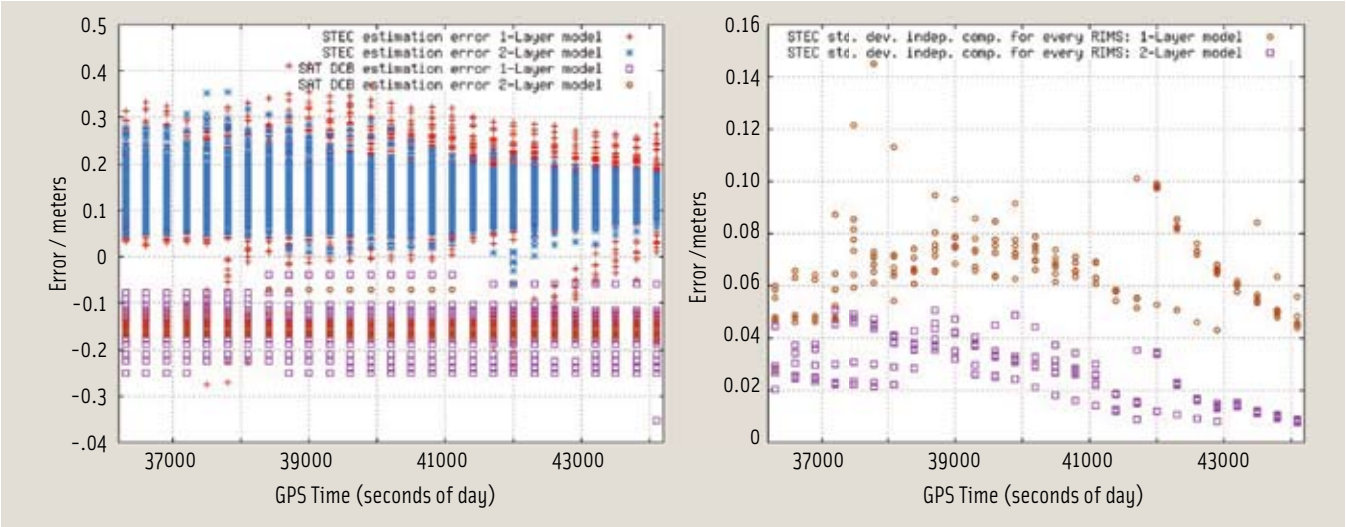

FIGURE 9 **Absolute slant total electron content (STEC) ionospheric delay and interfrequency delay code biases (DCBs) error for all the WARTK CPF data (left-hand plot), and standard deviation of the STEC per receiver (right-hand plot).**

(STEC) delay and interfrequency delay code bias (DCB) estimation, simultaneously solved with the remaining parameters at the CPF (left plot) The DCB can be mostly calculated from the ionospheric pseudorange, computed simultaneously with the TEC in this case.

Although the absolute error is on the order of 20 centimeters for STEC and is almost canceled out by the DCBs, the majority of this error is due to receiver bias. These biases are canceled out by double differencing.

This is clearly shown in the right-hand plot of Figure 9 where the standard deviation of the STEC error per receiver (not cancelled out in double differences) is few centimeters for the dual-layer ionospheric model.

We should note that WARTK does not require a high bandwidth for the transmission of the messages, compared to other carrier phase based navigation techniques. The WARTK method can use a low broadcast rate because the extra information in its broadcast messages (e.g., ionospheric corrections, DCBs, and ambiguities) take advantage of typically slow variations of the ionospheric electron content in a solar-magnetic reference frame.

Indeed, when we are not experiencing extreme solar activity, five-minute updates of Kalman filtering may be sufficient for our needs. A first estimate of the required bandwidth was less than few tens of kbps when only a single constellation is considered (such as GPS, see M. Hernández-Pajares et alia 2007b). In scenarios associated with peak solar activity conditions, an improvement of the temporal and spatial resolution may be needed, but this is not a problem, in particular from the point of view of the required computational load.

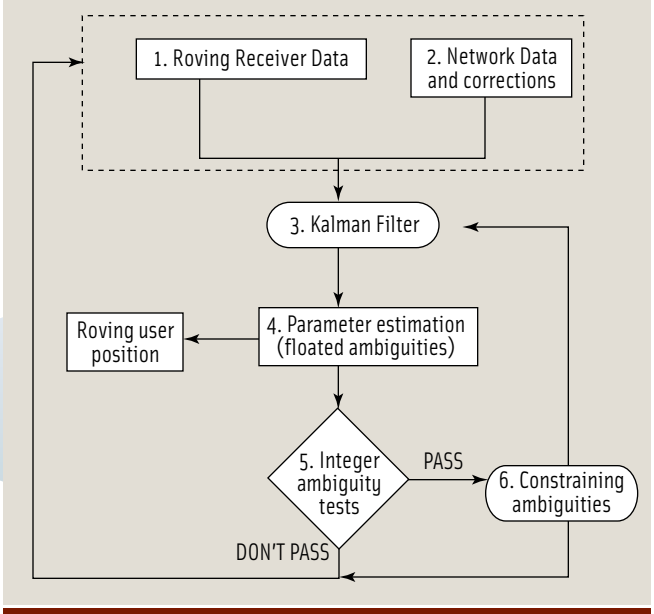

FIGURE 10 **WARTK algorithm layout for the user receiver**

WARTK User

As mentioned earlier, WARTK user navigation employs multi-frequency carrier phase data, combined with accurate corrections provided by the CPF, most importantly, ionospheric delay. With the ionospheric correction a user may add an extra equation to quickly estimate and fix the carrier phase ambiguities in real-time, as shown in **Figure 10**.

For a receiver making use of three or more frequencies, this process can be completed within a single epoch with a warm start, and, for a cold start, within the better part of a minute once the tropospheric delay has been estimated.

User receiver performance is also driven by the interpolation of the STEC values provided by the CPF for the corresponding satellite transmitter line of sight (LOS) to the permanent receivers. **Figure 11** illustrates that the error is below the threshold of 2.7 centimeters for almost all the cases, not only for quadratic fitting but also in the linear models. This result is also in agreement — in fact slightly better for the previ-

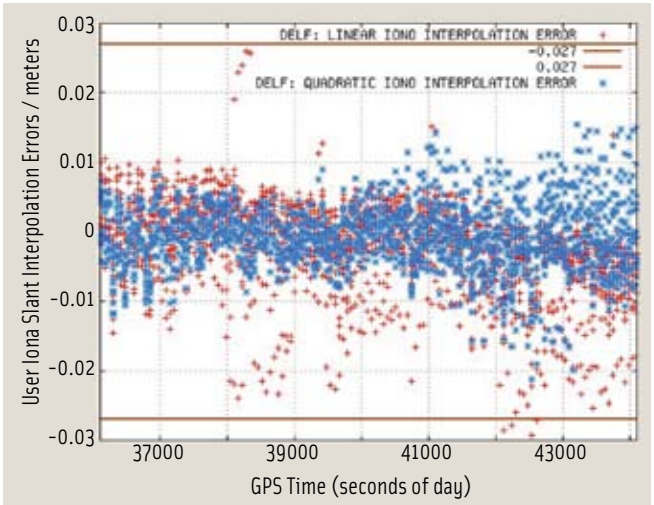

FIGURE 11 Slant ionospheric user error in terms of the time of the day in seconds, for the more distant roving users at Delft, comparing linear and quadratic fitting of the STEC values (corresponding to the WARTK permanent receivers, and broadcasted by the CPF).

ously mentioned reason — compared with the earlier results with actual GPS data (see for example Figure 7 from M. Hernández-Pajares et alia 2001).

WARTK user performance metrics, shown in **Figure 12**, include the positioning error and protection level, for vertical and horizontal components, in the case of full ambiguity fixing and dual constellation (left plots), as well as for a simulated single GPS constellation without ionospheric corrections, i.e., only ionospheric-free pseudorange and phase observations are used in the classical way (right plots).

The protection levels have been obtained empirically multiplying the formal standard deviation of the coordinates by 4.5 (equivalent to assume a post-fit Lc residual of 4.5 centimeters), and these values are enlarged by a Gaussian factor to try to ensure 10^{-7} for the vertical coordinate (factor of 5.3) and 10^{-9} (factor of 6.2) for the horizontal one.

Figure 12 illustrates the performance in two extreme cases in positioning: a user disposing only of GPS data, without ionospheric corrections and without fixing ambiguities, compared with positioning of a GPS+Galileo user disposing of precise real-time ionospheric corrections, and fixing carrier phase ambiguities.

In both cases a resetting each 600 seconds is performed to better characterize the performances.The usage of WARTK with a single GPS constellation produces an improvement of one to two orders of magnitude in both positioning error (at centimeter level) and protection level (at meter level). Notice that this result persists after resetting the user filter every 600 seconds, for the purpose of demonstrating WARTK performance after a user receiver cold start.

Figure 13 shows the convergence of positioning errors over time, also referred to as the user filter resetting time. Notice the improvement of up three orders by using the proposed technique. **Figure 14** depicts the convergence of the corresponding protection levels. Among the advantages of a multi-constellation over a single-constellation solution is the user's ability to fix both the wide and short-lane carrier phase ambiguities when the WARTK CPF provides real-time ionospheric corrections. Furthermore, the availability of three frequencies drives convergence almost to within a single-epoch (magenta and brown points), confirming the previously described results.

Notice in Figure 14 that the precise positioning convergence is realistic, but a little bit optimistic in particular for GPS data without ionospheric corrections (of the order of 600 second or slightly larger), compared with the actual case. But the relative performance between the classical and proposed approaches,

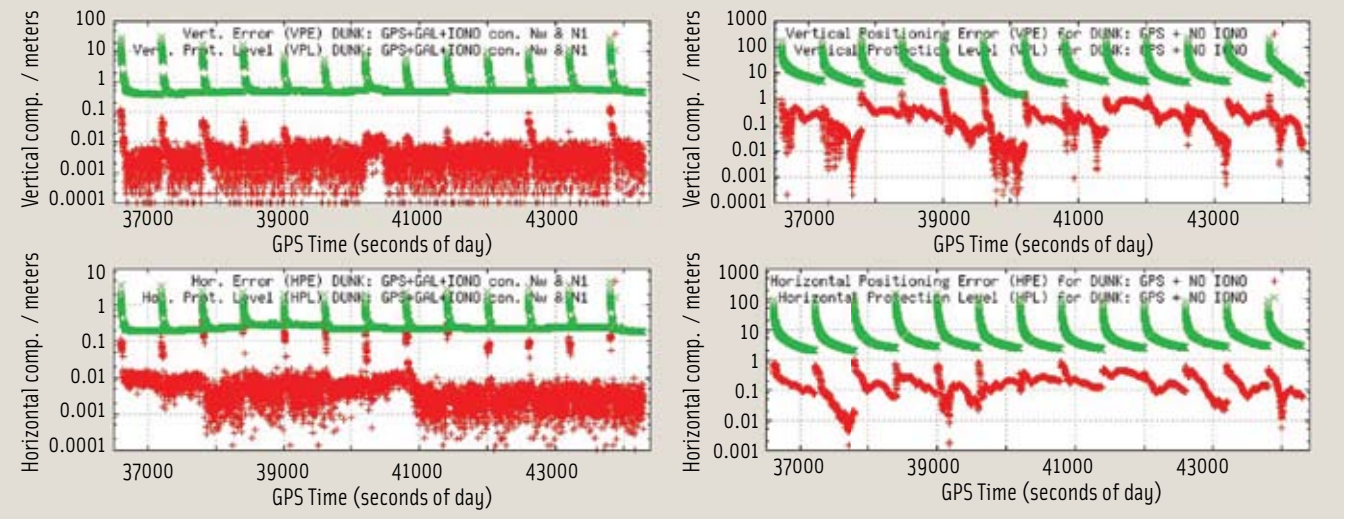

FIGURE 12 The WARTK user positioning error (red) and protection level (green) are represented with a dual constellation and full ambiguity fixing (left plots) versus classical approach, i.e., notusing ionospheric corrections and GPS constellation only (right plots), for both vertical and horizontal errors (top and bottom plots).

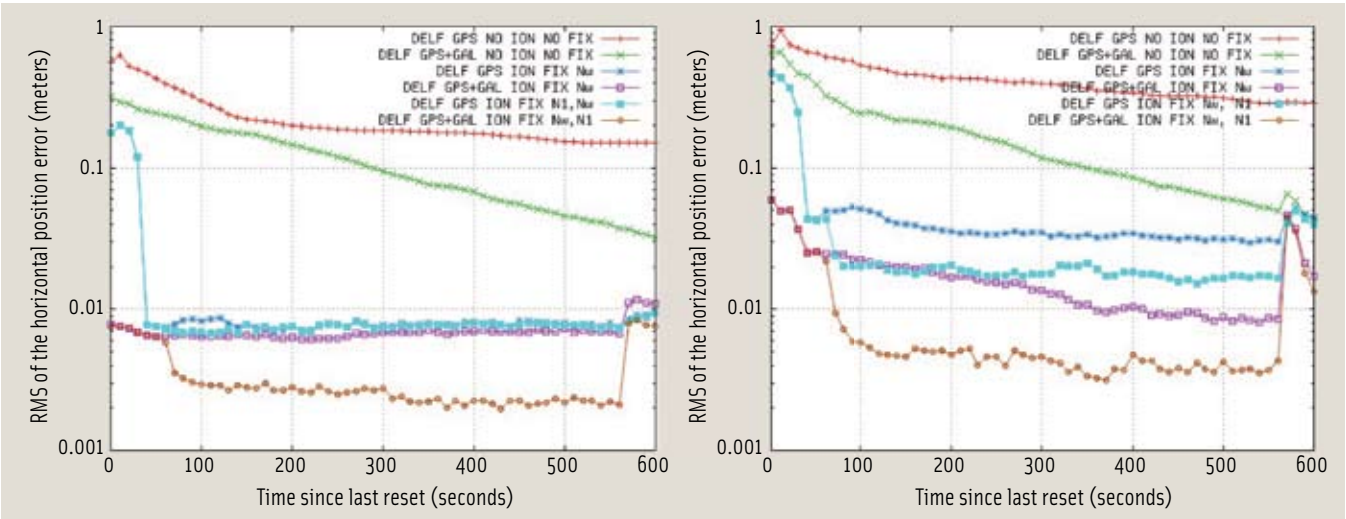

FIGURE 13 The convergence time of the averaged WARTK positioning errors for a roving user at Delft, for horizontal (left), and vertical (right) error, after the user filter reset. All runs are summarized here, resetting the user filter every 600 seconds. Various strategies are compared: Single constellation without using ionospheric corrections and without ambiguity fixing (red); Dual constellation with similar characteristics (green); Single and dual constellation with ionospheric corrections and fixing the wide-lane ambiguity only (blue and magenta respectively); and the corresponding calculations while fixing all the feasible ambiguities for wide and narrow lanes for GPS (light blue) and GPS+Galileo (brown).

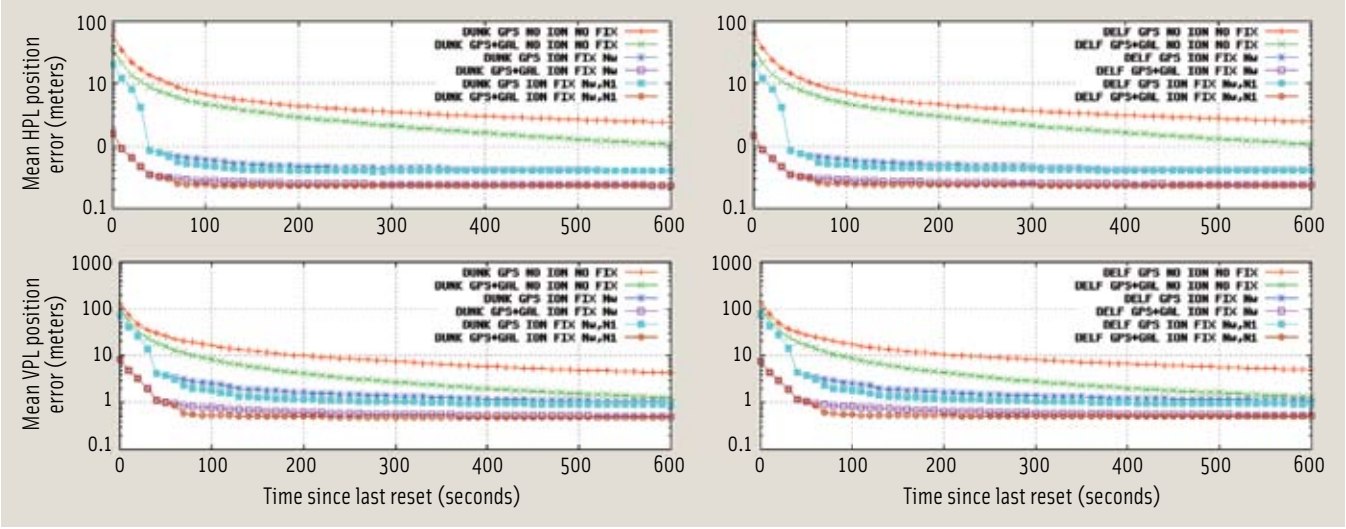

FIGURE 14 Vertical (top) and horizontal (bottom) protection levels (PL) for user DUNK (left) and DELF (right), corresponding to the different positioning strategies illustrated in previous figure (see corresponding caption for details).

for both single and dual constellation scenarios, is very clear and realistic, confirming previous studies involving actual and simulated data.

Finally, using Stanford plots for horizontal and vertical error components, **Figure 15** summarizes this experiment's WARTK user performance in terms of *misleading information* (MIs), which are points with higher actual errors or lower accuracy than the corresponding protection level — that is, instances where the integrity is missed due to a higher actual error than specified for a given horizontal or vertical protection level (HPL or VPL), caused by an MI.

Regarding the absence of MIs, the low protection levels in the simulated data are in agreement with results obtained for three months of actual data (See M. Hernández-Pajares et alia 2009).

Figure 16 presents the main experimental results of the WARTK performance. We want to particularly emphasize the drop in the 95th percentile levels of the horizontal and vertical positioning error (HPE and VPE). Despite the presence of ionospheric delay, these figures fall from 40 and 103 centimeters, when using regular carrier phase–based differential navigation to just 1.5 and 4 centimeters respectively, within 30 seconds after the user filter resets for the single GPS constellation.

The multi-constellation scenario notably improves the performance of the carrier phase–based differential user, but to a lesser extent. (HPE improves from 40 to 25 centimeters and VPE, from 103

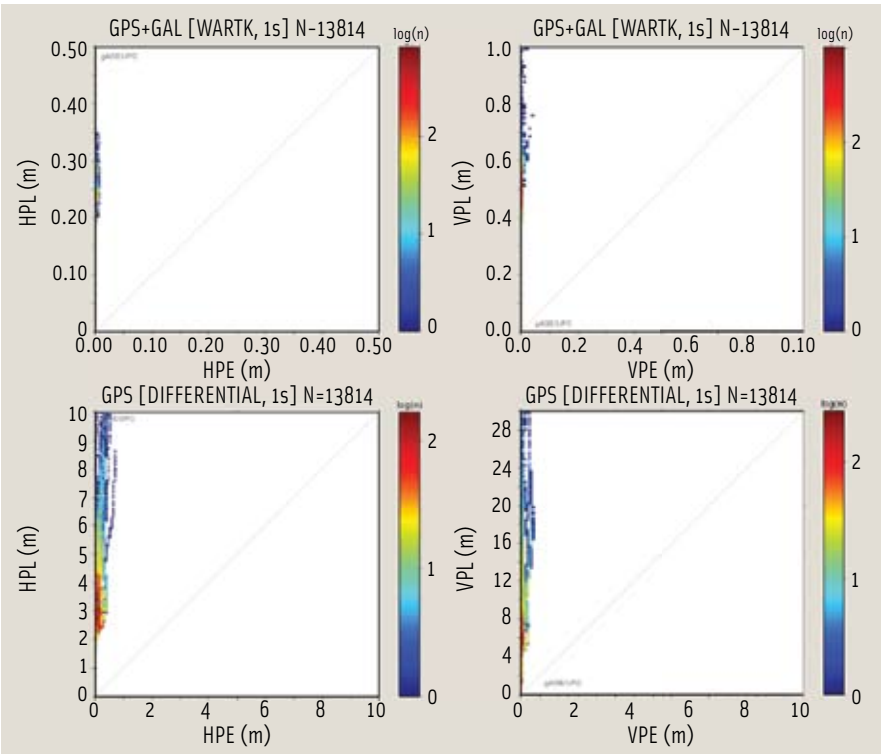

FIGURE 15 Stanford plots, showing the density of points per Accuracy x Protection level bins, for full ambiguity-fixing WARTK users. The horizontal protection level (HPL), left plots, and vertical protection level (VPL), right plots, are shown for the dual-constellation (GPS+Galileo) WARTK scenario (top row) and for a single-constellation (GPS) scenario using a plain carrier phase–based differential technique. Note the lack of *Misleading Information* events and correspondingly good integrity, as well as the low protection levels in the multi-constellation WARTK case.

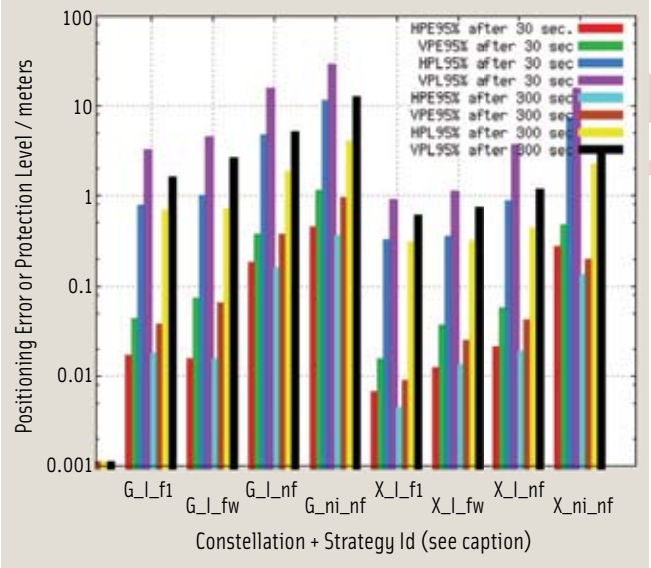

FIGURE 16 Summary of WARTK performance for Delft user, including horizontal positioning error (HPE), vertical positioning error (VPE), horizontal protection level (HPL) and vertical protection level (VPL), in millimeters (95 percent), after 30 and 300 seconds, illustrated in the first and second block of each set of four columns, respectively. This information is provided in different lines for the different user computation modes: G=GPS only, X=GPS+Galileo, I=using iono corrections, ni=not using them, f1=fixing L1 ambiguity, fw=fixing wide-lane ambiguity, nf=not fixing any ambiguity.

to 43 centimeters. The protection levels behave similarly, which are at 70 centimeters (HPL) and 289 centimeters (VPL) for a single (GPS) constellation, to less than one meter for each component in the dual constellation scenario, using the full WARTK ambiguity-fixing algorithm in both cases.

Single-Epoch Full Ambiguity Fixing with LAMBDA

In the previous results we have basically used a TCAR like approach for user ambiguity fixing. In fact, the double difference of the extra-wide lane (or just widelane for GPS), widelane and shortlane ambiguities are constrained to its integer value, in order to facilitate the usage of all the available observations, no just the ones with fixed ambiguities, to take the full profit of the GNSS satellites observing geometry.

In order to investigate the challenging single-epoch full-ambiguity resolution performance for the WARTK user, from the computations performed previously we applied the optimal mathematically well-founded LAMBDA method to the WARTK-corrected rover baselines to DUNK and DELF, as an add-on to the precise, real-time, ambiguity-fixing user algorithm described earlier.

To simulate cold start conditions, we applied the LAMBDA method in combination with the fixed-failure rate ratio test described in the article by P. J. G. Teunissen and S. Verhagen (Additional Resources) to the vector of double-differenced ambiguities obtained in single epoch mode. We set the fixed failure rate to 0.1% and entered the full vector of double-differenced ambiguities with no wide-lane or other ambiguity combinations formed *a priori*.

We then processed both user baselines, applying the precise ionospheric corrections received from the WARTK CPF and estimating a tropospheric zenith delay per epoch. Baselines were computed using dual-frequency (L1+L5) phase and code data of GPS only, and again using dual-frequency phase and code data of both GPS (L1+L5) and Galileo (L1+E5a) constellations.

The WARTK CPF results for the 257-kilometer baseline to DUNK produced a 92.3 percent success rate, for the 7,192 single epochs measured at one-second intervals. The integer ambiguities were correctly fixed by LAMBDA using GPS-only data from with five to eight satellites. Incorrect integer solutions were not accepted. Only 7.7 percent of the epochs did not pass the fixed failure-rate ratio test.

Because of this high success rate using GPS alone, the addition of Galileo only brought a marginal improvement from the perspective of ambiguity resolution: It increased to 100 percent using the multi-constellation data from 10-16 satellites.

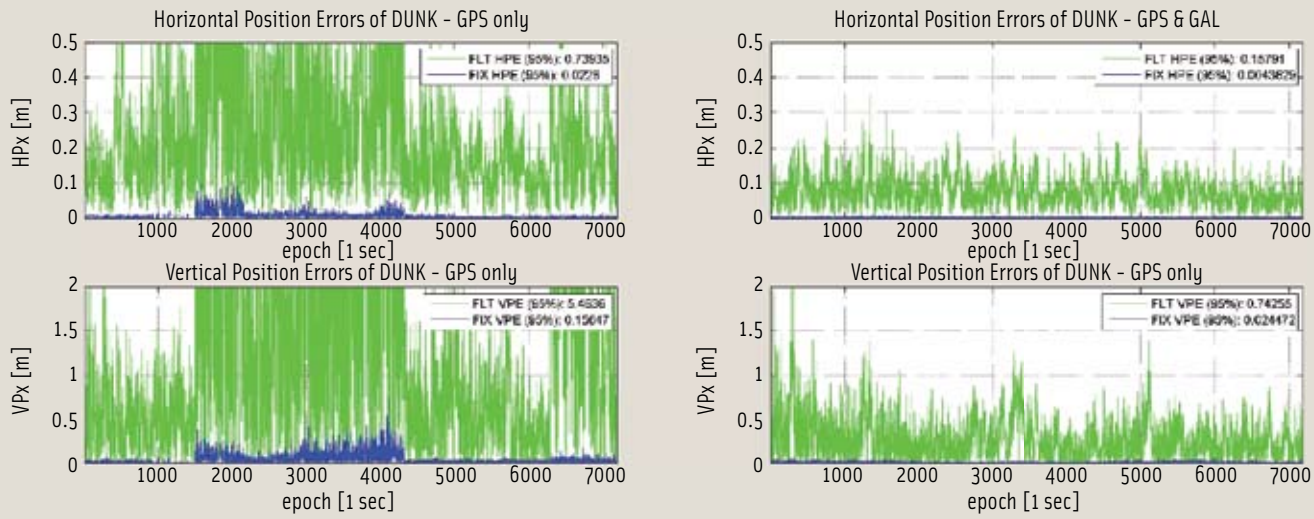

FIGURE 17 **Horizontal (top) and vertical (bottom) position errors for user DUNK, applying WARTK ionospheric corrections and single-epoch full LAMBDA-based dual-frequency ambiguity resolution. The graphs on the left show the float (green) and fixed (blue) position errors using GPS only, while those on the right show the multi-constellation position errors.**

However, the combination of GPS and Galileo improved the single-epoch precision of the rover position significantly. For example, by roughly doubling of the number of satellites, the float 95 percentile HPE reduced by almost a factor of five, while the fixed 95 percentile HPE decreased from 2.2 centimeters in the GPS-only case to 4 millimeters using GPS and Galileo data (see Figure 17).

We should point out that the single-epoch fixed-coordinate precision is mainly governed by the high precision of the phase data, and that in this study we have neglected some sub-centimeter effects, which could increase the error budget to one centimeter or more, in real-time precise geodetic modeling terms.

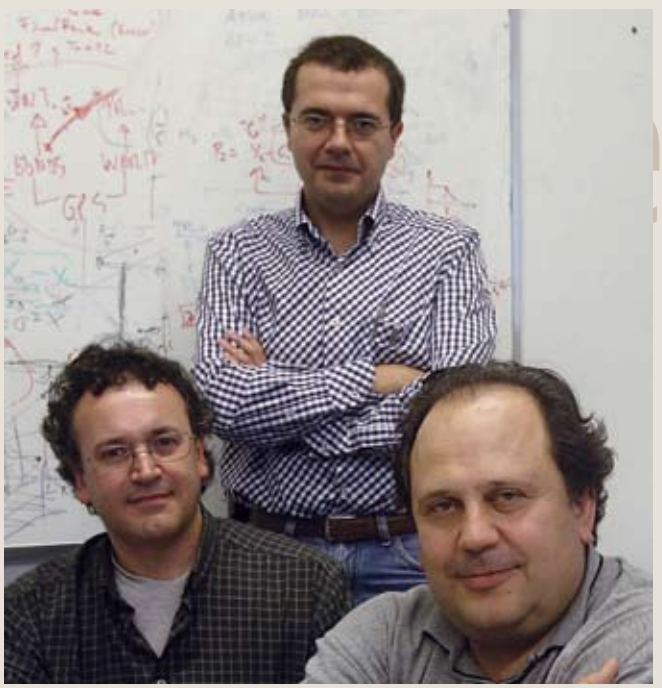

Manuel Hernández-Pajares (top), **J. Miguel Juan** (right), and **Jaume Sanz** (left) are associate professors at the Polytechnical University of Catalonia (UPC). Their current research interest is in the area of GPS ionospheric tomography, GPS data processing algorithms, satellite-based augmentation systems (SBAS) and precise radionavigation. They have recently founded the spin-off company gAGE-NAV S.L.

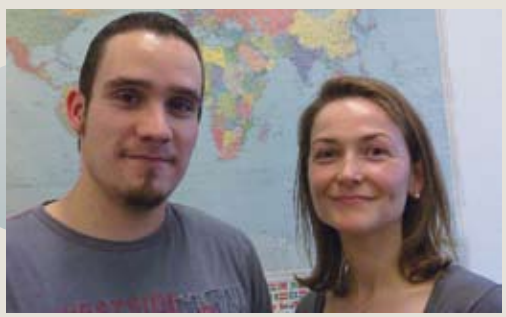

Angela Aragon-Angel (right) and **Pere Ramos-Bosch** (left) are researchers at the Technical University of Catalonia (UPC). Their working topics range from radio occultation to precise positioning and navigation within the area of GNSS data processing.

Dennis Odijk (right) is research fellow and **Peter Teunissen** (left) is professor in the new GNSS Research Lab of Curtin University of Technology, Australia. Before moving to Australia, they both worked at Delft University of Technology, where Peter Teunissen still holds a chair.

Figure 17 also shows that the position error becomes less sensitive to a change in number of satellites when many satellites are tracked. In the case of GPS-only data, some large position errors appear due to the weak satellite geometry based on using signals from only five or six satellites, and in this context a tropospheric zenith delay for each epoch is estimated in addition to the coordinate components.

For the 413-kilometer rover baseline to DELF the success rate of instantaneous LAMBDA-based ambiguity resolution using only GPS turned out to be much lower than for DUNK. In only 52 percent of the 7,192 epochs did the correct integers pass the fixed failure-rate ratio test. The epochs for which the ambiguity solutions did not pass the ratio test are mostly those with five to six satellites.

For this baseline, however, the addition of Galileo data improved LAMBDA-based full ambiguity resolution tremendously. The instantaneous success rate increased to 99.8 percent. The position errors of DELF for the case of combined GPS-Galileo data, are notably similar to the position errors of DUNK.

The processing of both user baselines demonstrates that successful single-epoch full LAMBDA-based ambiguity resolution is not feasible using GPS only, but requires a few minutes of initialization. However, we showed that the use of multi-constellation data increases the instantaneous LAMBDA-based ambiguity success rate to nearly 100 percent for both long baselines.

Conclusions

Our results confirm the maturity of the wide area real-time kinematic technique. Using a wide area permanent network of GNSS receivers, the technique provides not only outstanding accuracy at the decimeter level, but also integrity with protection levels of the order of one meter.

These results are typically achieved after a few minutes in the case of a dual-frequency single constellation user, or real scenario with GPS, and almost instantaneously with future three-frequency GNSS data, once the initial convergence of the user tropospheric delay is achieved. In both cases the WARTK technique also used the LAMBDA method to complete single-epoch real-time user carrier phase ambiguity fixing.

These results have been obtained with a GPS+Galileo receiver, gathering simultaneous simulated signals of Galileo and GPS satellites, and are being confirmed with large actual datasets in an on-going project.

Critical to the demonstration of these results, we acknowledge two key points: understanding the main factors influencing the estimation of the ionospheric delays (by the WARTK CPF) and transmitting these data to users (by means of the WARTK user interpolation method), and the use of optimal precise ionospheric and geodetic models and measurements at both the CPF and user levels in order to maximize the efficiency in real-time long-baseline carrier phase

Jaron Samson (top), **Michel Tossaint** (right) and **Michelangelo Albertazzi** (left) are radionavigation system engineers at the European Space Agency (ESTEC, The Netherlands). Samson and Albertazzi work for ESA's Technical Directorate, while Toussaint is a member of ESA's GNSS Evolutions team.

Peter de Bakker obtained his M.Sc.and has started as a Ph.D. candidate on the subject of precise point positioning and integrity monitoring, both at Delft University of Technology.

Sandra Verhagen obtained her Ph.D. and M.Sc. from Delft University of Technology and is now an assistant professor at the same university. Her research interests are carrier phase ambiguity resolution and quality control for real-time kinematic GNSS applications. Verhagen is president of International Association of Geodesy Commission 4 "Positioning and Applications."

Hans van der Marel is an assistant professor at Delft University of Technology, The Netherlands. He is involved in research on high precision GNSS positioning and navigation using GPS and Galileo, and scientific and meteorological applications of GNSS.

ambiguity fixing, and hence user accuracy and integrity. This can be done with an affordable bandwidth, especially by using the recently proposed space-state representation requiring a bandwidth of less than 600 bps for a single constellation, corresponding to 40 ground receivers tracking 30 satellites (M. Hernández-Pajares et alia, 2009b).

Moreover, we should note that the WARTK CPF may be used to support precise navigation while at the same time generating accurate real-time data products for many different user communities, including those with such interests as precise ionospheric models for space weather, instantaneous tropospheric delay determination for weather forecasting, and improvements in satellite clocks and orbits.

Manufacturers

The ESA/ESTEC test bench used a GSS7700 GPS/SBAS simulator and GSS7800 Galileo RF constellation simulator from **Spirent Communications plc**, Paignton, UK.

Additional Resources

[1] Agrotis L., IGS Real Time Pilot Project progress meeting, June 24, 2009

[2] Bilitza D., International Reference Ionosphere 2000, *Radio Science 36*, #2, pp. 261–275, 2001

[3] Colombo, O.L., and M. Hernández-Pajares, J. M. Juan, J. Sanz, and J. Talaya, "Resolving Carrier-Phase Ambiguities On the Fly, at More Than 100 km from Nearest Reference Site, with the Help of Ionospheric Tomography," Institute of Navigation ION GPS-99, Nashville, Tennessee, USA, September 1999

[4] Hernández-Pajares M., and J. M. Juan, J. Sanz and O.L. Colombo (1999a), "Precise Ionospheric Determination and its Application to Real-Time GPS Ambiguity Resolution," Institute of Navigation ION GPS-99, Nashville, Tennessee, USA, September 1999

[5] Hernández-Pajares M., and J. M. Juan, J. Sanz (1999b), "New Approaches in Global Ionospheric Determination Using Ground GPS Data," *Journal of Atmospheric and Solar-Terrestrial Physics 61*, pp. 1237-1247,1999

[6] Hernández-Pajares, M., and J. M. Juan, J. Sanz, and O.L. Colombo, "Application of Ionospheric Tomography to Real-Time GPS Carrier-Phase Ambiguities Resolution, at Scales of 400–1000 km, and with High Geomagnetic Activity," *Geophysical Research Letters*, 27, pp. 2009-2012, 2000.

[7] Hernández-Pajares, M., J.M. Juan, J. Sanz and O.L. Colombo (2001), "Tomographic modeling of GNSS ionospheric corrections: Assessment and real-time applications", ION GPS-2001, Salt-Lake, Utah, USA, September 2001.

[8] Hernández-Pajares, M., and J. M. Juan, J. Sanz, and O.L. Colombo, "Improving the Real-Time Ionospheric Determination from GPS Sites at Very Long Distances over the Equator," *Journal of Geophysical Research*, V.107, No. A10, 1296, 2002

[9] Hernández-Pajares, M., and J. M. Juan, J. Sanz, and O.L. Colombo, "Feasibility of Wide-Area Subdecimeter Navigation with GALILEO and Modernized GPS," *IEEE Transactions on Geoscience and Remote Sensing*, V. 41, No. 9, 2003

[10] Hernández-Pajares, M., and J. M. Juan, J. Sanz, A. García-Rodríguez, and O.L. Colombo, "Wide Area Real Time Kinematics with Galileo and GPS Signals," ION GNSS-2004, Long Beach, California, USA, September 2004

[11] Hernandez-Pajares M., and J.M. Juan, J. Sanz (2006a), "Medium Scale Traveling Disturbances Affecting GPS Measurements: Spatial and Temporal Analysis," *Journal of Gephysical Research*, doi:10.1029/2005JA011471, Vol. 111, A07 S11, 2006

[12] Hernandez-Pajares, M., and J.M. Juan, and J. Sanz (2006b), Real time MSTIDs modelling and application to improve the precise GPS and GALILEO navigation, *Proceeedings of ION GNSS-2006, September 2006*

[13] Hernández-Pajares, M., and J. M. Juan, J. Sanz, A. García-Rigo, R. Chen, X. Li, J. Talaya, E. Bosch, T. Schueler, E. Schueler, S. Soley, and M. Reche, "WARTK-EGAL: WARTK Based on EGNOS and Galileo: Technical Feasibility Study," invited presentation at Growing Galileo Conference & Exhibition, European GNSS Supervisory Authority, Brussels, November 14–15, 2007

[14] Hernández-Pajares, M., and J. M. Juan, J. Sanz, A. Aragón-Angel, P. Ramos-Bosch, D. Odijk, P. F. de Bakker, H. van der Marel, S. Verhagen, I. Fernández-Hernández, M. Toledo, and J. Samson, "TN3.1: WARTK Algorithms and messages at PF level", page 60, report of the project "Feasibility study of a Wide Area High-precision Navigation Service (WARTK) for EGNOS & Galileo (FES-WARTK)", funded by ESA, September 2007b.

[15] Hernández-Pajares, M., and J. M. Juan, J. Sanz, A. Aragón-Angel, P. Ramos-Bosch, D. Odijk, P. F. de Bakker, H. van der Marel, S. Verhagen, I. Fernández-Hernández, M. Toledo, and J. Samson, "Feasibility Study of a European Wide Area Real Time Kinematic System," invited talk in 4th ESA Workshop on Satellite Navigation User Equipment Technologies (Navitec), ESTEC, Noordwijk, The Netherlands, December 2008

[16] Hernández-Pajares, M., and J. M. Juan, J. Sanz (2009a), "WARTK Evaluation with Real GPS Data Report (GNSS-MRS-TN-UPC-I-070001)," within the ESA GNSS Evolution MRS project, presented at the MRS Progress Meeting, Barcelona, Spain, July 23, 2009

[17] Hernández-Pajares, M., and J. M. Juan, J. Sanz (2009b), UPC Contribution to Enhanced Precise Point Positioning (EPPP) Progress Meeting Number 4, Barcelona, Spain, December 3, 2009

[18] Juan, J.M., and P. Ramos (2009), Techical Notes #2 and #3: "GPS PRTODTS Design and Validation Documents" of ESA funded "Precise Real-time Orbits and Clocks Determination" (PRTODTS) project, Barcelona, December 2009.

[19] Simsky, A., and D. Mertens, J-M. Sleewaegen, W. de Wilde, M. Hollreiser, and M. Crisci, "MBOC vs. BOC(1,1) Multipath Comparison Based on GIOVE-B Data," *Inside GNSS*, pp. 36–40, September/October 2008

[20] Teunissen, P. J. G., (1995), "The Least-Squares Ambiguity Decorrelation Adjustment: a Method for Fast GPS Integer Ambiguity Resolution" *Journal of Geodesy*, 70(1-2): 65-82

[21] Teunissen, P. J. G., (1999): A Theorem on Maximizing the Probability of Correct Integer Estimation," *Artificial Satellites*, 34(1), pp. 3-9

[22] Teunissen, P.J.G., and S. Verhagen, "The GNSS Ambiguity Ratio-Test Revisited," *Survey Review*, Vol. 41, No. 312, pp. 138-151, 2009

[23] Wanninger, L., "Introduction to Network RTK," from <http://www.network.info/intro/introduction.html> 2008 IG